




AKADÉMIAI KIADÓ

Nonlinear control of wind turbine in above rated wind speed region

El Kabira El Mjabber^{1*} , Abdellatif Khamlichi² and Abdellah El Hajjaji¹

¹ Department of Physics, Faculty of Sciences, University Abdelmalek Essaadi, 93030 Tetouan, Morocco

² Department of Industrial and Civil Sciences and Technologies, National School of Applied Sciences, University Abdelmalek Essaadi, 93030 Tetouan, Morocco

Received: February 15, 2021 • Revised manuscript received: May 22, 2021 • Accepted: May 25, 2021
Published online: November 8, 2021

Pollack Periodica •
An International Journal
for Engineering and
Information Sciences

17 (2022) 1, 72-77

DOI:
[10.1556/606.2021.00411](https://doi.org/10.1556/606.2021.00411)
© 2021 Akadémiai Kiadó, Budapest

ORIGINAL RESEARCH
PAPER



ABSTRACT

Advanced control of variable speed horizontal wind turbine was considered in the high wind speed range. The aims of control in this region are to limit and stabilize the rotor speed and electrical power to their nominal values, while reducing the fatigue loads acting on the structure. A new nonlinear technique based on combination between sliding mode control and radial basis function neural network control was investigated. The proposed hybrid controller was implemented via MATLAB on a simplified two masses numerical model of wind turbine. By applying the Lyapunov approach, this controller was shown to ensure stability. It was found also to be robust and able to reject the uncertainties associated to system nonlinearities. The obtained results were compared with those provided by an existing controller.

KEYWORDS

nonlinear control, pitch angle, sliding mode control, radial basis function

1. INTRODUCTION

A wind turbine is a machine compound of several sub-systems that has the principal role of extracting energy from the wind. The main objective of a wind turbine controller is to optimize this energy extraction and ensure that it is performed safely without damaging the wind turbine structure. Much attention has been given, over the past few decades, to blade pitch control systems in the region 3, where the wind speed is higher than the rated value. This operating region is called the above rated wind speed [1]. Pitch control consists of rotating the blades around their longitudinal axis on the rotor hub. Therefore, pitching the blades (tuning) gradually out of the wind extends to limit the captured aerodynamic torque and thus to keep the production power around its nominal value. Pitch control should be performed while also minimizing mechanical fatigue loads and torque oscillations amplitude of the electric generator [2, 3].

Several approaches have been investigated in the literature to improve pitch control performance. Several researchers have developed various adaptive controllers. These techniques used at the beginning classical methods, such as linear Proportional Integral Derivative (PID) based control [4, 5]. However, the nonlinear state of a wind turbine requires the intervention of other advanced controllers that can facilitate better the control. For instance, Radial Basic Function (RBF) combined with PID was used to control the pitch angle [6]. Other adaptive controllers based on methods like artificial intelligence, back-stepping [7], L_1 approach, and sliding mode [8] were also introduced. Sliding Mode Controller (SMC) was widely used to control nonlinear systems with disturbances due to its robustness and stability against the perturbations affecting the dynamics of these systems [9]. However, the SMC

*Corresponding author.
E-mail: kabira.mjabber@gmail.com

suffers from the undesired large control chattering phenomenon which is caused by the large switching gain of the discontinuous switching control term [10, 11]. Thus, an additional disturbance due to the controller itself was added to the system. Therefore, it has been sought to remedy against this major drawback of SMC controller by proposing to pair it with another controller. A multi-variable control strategy for variable speed and variable pitch angle wind turbine has then been investigated in several works [2, 12].

In this paper, the choice has been set on the Radial Basis Function Neural Network (RBFNN) to be combined to Integral Sliding Mode Control (ISMC). The resulting new controller designated (ISMC-RBF) will be investigated. The main pursued challenge of this hybrid controller is to benefit from the RBFNN protocol, which is known to enable accurate estimation of the systems nonlinearities, in order to reduce system uncertainties. It is also aimed to profit from the robustness of SMC protocol. The goal is in fact to take advantages from these two beneficial aspects towards minimizing the chattering effects and to achieve better efficiency of control. This technique was developed in this work to control a wind turbine modeled as a 2-mass system in the region 3. The proposed controller aims to keep rotor speed and electrical power at their nominal values while stabilizing the generated electrical power and reducing mechanical load fluctuations.

2. MATERIALS AND METHOD

2.1. Wind turbine modeling

Wind energy is exploited through a converter system that is utilized to convert the wind kinetic energy into mechanical power by means of the rotor blades which is set vertical and orthogonal to the wind direction. The mechanical energy is then carried through the drive train and converted into electrical energy. This step of conversion is carried out across the electrical system, which consists of electrical generator and electronic power converter. This kind of wind turbine is called horizontal axis wind turbine and constitutes the subject of the modeling and control that will be presented in the following.

The aerodynamic power extracted from the air by wind turbine rotor can be expressed in terms of air density ρ and wind speed v by the flowing equation [13]:

$$P_a = \frac{1}{2} \rho \pi R^2 C_p v(t)^3, \quad (1)$$

where R is the wind turbine radius and C_p depicts the power coefficient. C_p has a nonlinear behavior since it depends on pitch angle β and tip speed ratio λ .

The aerodynamic rotor deduced from the relationship $P_a = T_a \omega_t$ takes the flowing form:

$$T_a = \frac{\rho \pi R^2}{2} \frac{C_p(\lambda, \beta)}{\omega_t} v^3, \quad (2)$$

where ω_t denotes the rotation speed of the blades.

The dynamic behavior of generator and rotor; as presented by a two-mass model are given by

$$\begin{cases} \dot{\omega}_g = \frac{T_{hs}}{J_g} - \frac{K_g}{J_g} \omega_g - \frac{T_{em}}{J_g}, \\ \dot{\omega}_t = \frac{T_a}{J_r} - \frac{T_{ls}}{J_r} - \frac{K_r}{J_r} \omega_t, \end{cases} \quad (3)$$

where T_{ls} and T_{hs} are the low and high speeds shaft torques respectively T_{em} depicts the electromagnetic torque; K_r , and K_g are the external damping; ω_g is the generator speed; J_r and J_g are the rotor and generator inertia respectively. The relationship between T_{ls} , T_{hs} and ω_t , ω_g is determined by the gearbox ratio n_g :

$$n_g = \frac{T_{ls}}{T_{hs}} = \frac{\omega_g}{\omega_t}. \quad (4)$$

The torque T_{ls} can be expressed as function of the difference between angular rotor speed ω_t and that of the output shaft at its endpoint on the gearbox side, denoted ω_{ls} , and of the difference between the rotor angular position θ_t and that of the output shaft at its other end θ_{ls} , [13]:

$$T_{ls} = B_{ls}(\theta_t - \theta_{ls}) + K_{ls}(\omega_t - \omega_{ls}), \quad (5)$$

where B_{ls} is the low-speed shaft stiffness and K_{ls} represents the external damping.

2.2. Integral sliding mode control

The two-mass model requires control that is able to deal with other hidden functions that are not integrated explicitly into the simplified numerical model. Since the basic SMC has limitations in saturation that can cause instability or divergence in the system output, integral control is introduced to make it easier for the system to meet the desired objectives. The sliding surface is then chosen as:

$$S(t) = \dot{e}_p(t) + \delta e_p(t) + G \int_0^t e_p(t) dt, \quad (6)$$

where δ and G are positive constants. The tracking error e_p is applied to electrical power:

$$e_p = P_{ref} - P_e, \quad (7)$$

where P_{ref} takes the nominal value, which is equal to 600 kW in this paper. The generator losses are neglected. The electrical power has the form:

$$P_e = T_{em} \omega_g. \quad (8)$$

Taking the time derivative of the electrical power as given in (8), the following can be obtained:

$$\dot{P}_e = \dot{\omega}_g T_{em} + \omega_g \dot{T}_{em}. \quad (9)$$

To improve the stability of the system, the attraction of the sliding surface S is determined by the Lyapunov criterion, which is called the reachability condition [10]:

$$\dot{S} < 0. \quad (10)$$

The control of nonlinear system is taken under the following general form:



$$\dot{x} = f + gu + d. \quad (11)$$

According to (3) and (9), the parameters in (11) can be obtained by the following equations:

$$\begin{cases} x = P_e, \\ f = \omega_g \dot{T}_{em}, \\ g = \frac{T_{hs}}{J_g} - \frac{K_g}{J_g} - \frac{T_{em}}{J_g}, \\ u = T_{em}. \end{cases} \quad (12)$$

There are two steps in the SMC design. The first one requires calculating equivalent law control u_{eq} through the Lyapunov stability theory. The second one leads to the construction of the switched control part u_{sw} that is necessary to drive the system trajectory to vary on the sliding surface. The global SMC law can be obtained as [10]:

$$u = u_{eq} + u_{sw}. \quad (13)$$

When the sliding surface is reached $S = 0$, which can result in, $\dot{e}_p(t) + \delta e_p(t) + G \int_0^t e_p(t) dt = 0$ the system is said to be asymptotically stable, therefore $e_p \rightarrow 0$ and $\dot{e}_p \rightarrow 0$. The particular case $S = 0$ is selected for the reason that it has a suitable reduced-order dynamics. The condition of convergence is given by the equation of Lyapunov $V \dot{\leq} 0$, which makes the sliding surface to be attractive and invariable.

By using (4) and (5), and applying the condition $S = 0$:

$$\ddot{e}_p(t) + \delta(\dot{P}_{ref} - \dot{P}_e(t)) + Ge_p(t) = 0. \quad (14)$$

Since the reference, power P_{ref} is constant and then its derivative is zero $\dot{P}_{ref} = 0$.

To deduce the command input, the term $\dot{P}_e(t)$ is substituted in Eq. (15) by its expression defined by Eqs (11) and (12) which leads to:

$$u_{eq} = \frac{1}{g} \left(\frac{1}{\delta} \ddot{e}(t) + \frac{G}{\delta \omega_g} e_p(t) - f(\omega_g) \right). \quad (15)$$

In order to reach the sliding mode condition (10) and decrease chattering, the signum function (sign) is used instead on switch function $u_{sw} = \eta \text{sign}(S)$.

The control law leads to the following final form:

$$\begin{aligned} u &= u_{eq} + u_{sw} \\ &= \frac{1}{g} \left(\frac{1}{\delta} \ddot{e}(t) + \frac{G}{\delta \omega_g} e_p(t) - f(\omega_g) + \eta \text{sign}(S) \right). \end{aligned} \quad (16)$$

When $f(\cdot)$ is uncertain, RBFNN can be used to learn and approximate better $f(\cdot)$.

2.3. Adaptive nonlinear controller-based on SMC and RBF

The RBF was extensively applied in many fields for control and approximation. It can be also applied to model any complicated nonlinear function. RBF includes three layers.

The input layer consists of the input variable x_i , the hidden layer that contains the activation functions ψ_j , and the output layer consists of one node f_r . Therefore, RBF neural networks are chosen in this paper for their ability to approximate nonlinear functions. The radial basis function output is determined by [14]:

$$f_r(t) = \sum_{j=1} w_{ij} \psi_j(t), \quad i = 1, \dots, n, \quad (17)$$

where i is the input number of the network, j is the number of hidden layer nodes in the network. The activation function ψ_j is a Gaussian function presented in the following form [14]:

$$\psi_j(t) = \exp \left[-\frac{\|x(t) - C_j(t)\|^2}{2b_j^2} \right], \quad j = 1, \dots, N, \quad (18)$$

where N denotes the number of hidden layer nodes.

By using the general nonlinear form (11), the dynamic equation of RBFNN is:

$$\dot{P}_e = f(\omega_g, \dot{T}_{em}) + g(T_{ls}, T_{em})u + d, \quad (19)$$

where $f(\omega_g, \dot{T}_{em}) = \omega_g \dot{T}_{em}$ and $g(T_{ls}, T_{em}) = \frac{T_{ls}}{n_g J_g} - \frac{K_g}{J_g} \omega_g - \frac{T_{em}}{J_g}$.

To extract the control law $u = T_{em}$, a second-order dynamic is imposed to the tracking error (7):

$$\ddot{e}_p(t) + \delta \dot{e}_p(t) + Ge_p = 0. \quad (20)$$

Applying now Laplace transformation on (20), the following can be obtained: $p^2 + \delta p + G$. To ensure equilibrium stability, the polynomial $p^2 + \delta p + G$ must be Hurwitz.

According to (7) and (20), the equation of power dynamic is extracted as:

$$\dot{P}_e = \frac{1}{\delta} \left(-\ddot{P}_e + Ge_p \right). \quad (21)$$

By using (19) and (21), the following equation is obtained:

$$\begin{aligned} &f(\omega_g, \dot{T}_{em}) + g(T_{ls}, T_{em})u + d \\ &= \frac{1}{\delta} \left(-\ddot{P}_e + Ge_p(t) \right). \end{aligned} \quad (22)$$

By using (22), the law control is deduced as:

$$u = \frac{1}{g(T_{ls}, T_{em})} \left[\frac{1}{\delta} \left(\ddot{P}_e - Ge_p \right) + f(\omega_g, \dot{T}_{em}) + d \right]. \quad (23)$$

The functions $f(\omega_g, \dot{T}_{em})$ and $g(T_{ls}, T_{em})$ are highly complex and should be assumed to be uncertain nonlinear functions. They are functions of dynamic torque \dot{T}_{em} and torque T_{ls} and the generator speed ω_g . They depend



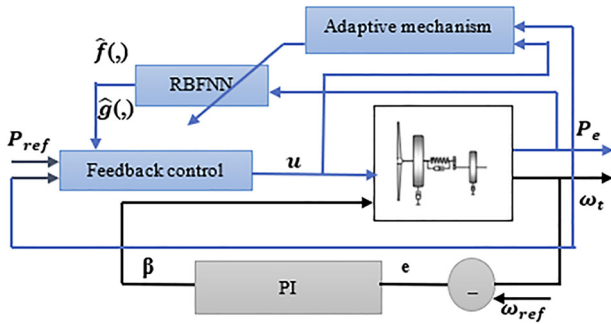


Fig. 1. Block scheme of multivariable control

implicitly as well on rotor speed ω_t , the power coefficient C_p , and wind speed v . Therefore, the control difficulty increases and controller efficiency decreases if inadequate approximations of these functions are used. In our case, two RBF neural networks will be proposed to approximate $f(\cdot)$ and $g(\cdot)$ functions. The system control is considered to be a closed-loop adaptive scheme that is illustrated in Fig. 1. By using (17) and (18), $f(\omega_g, \dot{T}_{em})$ and $g(T_{ls}, T_{em})$ will be approximated respectively as $f(\cdot) = W^{*T} \psi_f(x) + e_f$ and $g(\cdot) = V^{*T} \psi_g(x) + e_g$, where the items $f(\cdot)$ and $g(\cdot)$ are the ideal output value of the network, W^* and V^* are the ideal weights of the neural network, e_f and e_g are the approximation error of the neural network, which are bounded as $|e_f| \leq e_{fM}$, $|e_g| \leq e_{gM}$. The estimated RBF output can be presented as: $\hat{f}(x) = \hat{W}^T \psi_f(x)$, $\hat{g}(x) = \hat{V}^T \psi_g(x)$ with $d\hat{W}/dt = -(1/\gamma)e\psi(e)$.

Finally, the control law becomes:

$$\hat{u} = \frac{1}{\hat{g}(T_{ls}, T_{em})} \left[\frac{1}{\delta} (\ddot{P}_e - Ge_p) + \hat{f}(\omega_g, \dot{T}_{em}) \right] + \eta \text{sign}(S). \quad (24)$$

Stability proof:

$$V = \frac{1}{2} \gamma_3 \tilde{W}^T \tilde{W} + \frac{1}{2} \gamma_4 \tilde{V}^T \tilde{V} + \frac{1}{2} S^2, \quad (25)$$

with $\tilde{W} = W - \hat{W}$, $\gamma_3 > 0$ and $\tilde{V} = V - \hat{V}$, $\gamma_4 > 0$.

The time derivative of (25) gives:

$$\dot{V} = \gamma_3 \tilde{W}^T \dot{\tilde{W}} + \frac{1}{2} \gamma_4 \tilde{V}^T \dot{\tilde{V}} + S\dot{S}. \quad (26)$$

by substituting the time derivative of (6) into (26) one can obtain

$$\dot{V} = \gamma_3 \tilde{W}^T \dot{\tilde{W}} + \frac{1}{2} \gamma_4 \tilde{V}^T \dot{\tilde{V}} + S(\ddot{e}_p - \delta \dot{P}_e + Ge_p). \quad (27)$$

Let's take $\aleph(W, V) = \gamma_3 \tilde{W}^T \dot{\tilde{W}} + \frac{1}{2} \gamma_4 \tilde{V}^T \dot{\tilde{V}}$ and $f_l = \ddot{e}_p - \delta \dot{P}_e$.

Using now (19) to replace \dot{P} into (27):

$$\dot{V} = \aleph + S(\ddot{e}_p - \delta \dot{f} - \delta g_u - \delta d + Ge_p), \quad (28)$$

$$\dot{V} = \aleph + S \begin{pmatrix} f_l - \delta g_u + \delta \hat{g}_u - \\ -\delta \hat{g}_u - \delta d + Ge_p \end{pmatrix}, \quad (29)$$

$$\dot{V} = \aleph + S \begin{pmatrix} f_l - \delta u(g - \hat{g}) - \\ -\delta d + Ge_p \end{pmatrix} - \delta \hat{g} \frac{S}{\hat{g}(\cdot)} \begin{bmatrix} -\frac{1}{\delta} (\ddot{P}_e - Ge_p) - \\ -\hat{f}(\cdot) - \eta \text{sign}(S) \end{bmatrix}, \quad (30)$$

$$\dot{V} = \aleph + S(\delta \tilde{f} + \delta u \tilde{g} - \delta d), \quad (31)$$

where $\tilde{f} = \hat{f} - f = \tilde{W} \psi_f - e_f$, $\tilde{g} = \hat{g} - g = \tilde{V} \psi_g - e_g$.

Then:

$$\dot{V} = \tilde{W}^T (S \delta \psi_f - \gamma_3 \dot{\tilde{W}}) + \tilde{V}^T (S \delta u \psi_g - \gamma_4 \dot{\tilde{V}}) - S \delta e_f - S \delta u e_g - S \delta d - \eta |\text{sign}(S)| \leq 0 \quad (32)$$

with $\lim_{t \rightarrow \infty} |S(t)| = 0$ and by imposing the Lyapunov conditions of stability the weights W and V are given by:

$$\begin{aligned} \dot{\tilde{W}} &= \frac{1}{\gamma_3} S \delta \psi_f, \\ \dot{\tilde{V}} &= \frac{1}{\gamma_4} S \delta u \psi_g. \end{aligned} \quad (33)$$

2.4. Pitch angle control

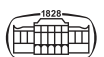
When the wind speed is greater than the nominal value, the torque control output is set to its nominal value, which then constitutes the maximum value of the control input. In this work, a linear control of the pitch angle using a PI controller is used to maintain the speed of the generator around its nominal value. The implementation of this controller does not require sophisticated means in the industrial context. The general form of PI control is given by:

$$\dot{\beta} = K_p \dot{e} + K_i e \quad (34)$$

with K_p and K_i are positive constants. The tracking error is of the form: $e = \omega_{ref} - \omega_t$, where ω_{ref} represents the nominal rotor speed. Figure 1 shows the block diagram of the multivariable control in both torque and pitch that is proposed in this work:

3. RESULTS AND DISCUSSION

In this work, the performances of the proposed and developed control method are studied by using numerical simulations on the Controls Advanced Research Turbine (CART)



[15]. CART is a variable speed wind turbine, variable pitch, two-bladed, and flexible hub. Its nominal power is 600 kW and other characteristics are presented in Table 1 [15]. To test the performance of the proposed hybrid controller ISMC-RBF, a comparison is made with the following reference controllers: ISMC [10] and RBFNN.

The von Karman model is used to generate the input wind speed. Figure 2 shows wind variations where turbulence was treated as a stationary random process. The wind simulation shows variations in the form of a noise-ranging from 15.7 m s^{-1} to 18 m s^{-1} .

The variation of rotor speed ω_t is given by Fig. 3. The comparison between ISMC-RBF and ISMC controllers shows that $\omega_{t_{ISMPRBF}}$ fluctuations are more satisfactory than those of $\omega_{t_{ISMC}}$.

The obtained STandard Deviation (STD) is in the case of the ISMC $std(\omega_{t_{ISMC}})=1.31$ and only $std(\omega_{t_{ISMCRBF}})=1.02$ for the hybrid controller, (Table 2). Among the main control objectives for the high wind speed is to keep the rotor speed closer to its nominal value. As it can be seen in Table 2, the maximum value of rotor speed $\omega_{t_{ISMC}}$ is 61.6 rpm, which is more unfavorable than the maximum rotor speed $\omega_{t_{ISMCRBF}}$, associated to the hybrid controller which does not exceed 59 rpm. Figure 4 shows variations of electrical power. According to the simulation, it is clear that the electrical power given by the proposed controller is around the nominal value 600 kW contrary to

the ISMC, which predicts a static excess of power that can harm the generator.

The pitch angle β variation shown in Fig. 5 is similar for both controllers. However, the ISMC-RBF deviations are lesser than those of ISMC controller.

The comparison of electromagnetic torque performance is given in Table 3. The result obtained by ISMC controller shows important deviation for ISMC for which the calculated STD value is 0.088 kN.m, and only

Table 1. Wind turbine parameters

Wind turbine parameter	Value	Unit
Rotor diameter	21.65	m
Air density	1.29	kg m^{-3}
Gearbox ratio	36.6	m
Shaft damping coefficient	9,500	$\text{N.m rad}^{-1}\text{s}^{-1}$
Shaft stiffness coefficient	$2.691 \cdot 10^5$	N.m rad^{-1}
Rotor friction coefficient	27.36	$\text{N.m rad}^{-1}\text{s}^{-1}$
Generator friction coefficient	0.2	$\text{N.m rad}^{-1}\text{s}^{-1}$

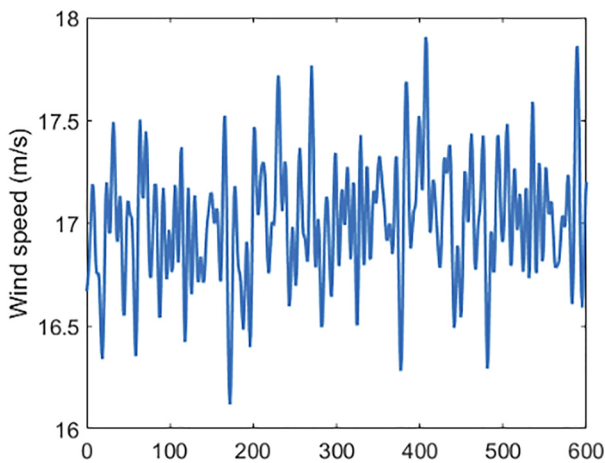


Fig. 2. Time variations of wind speed

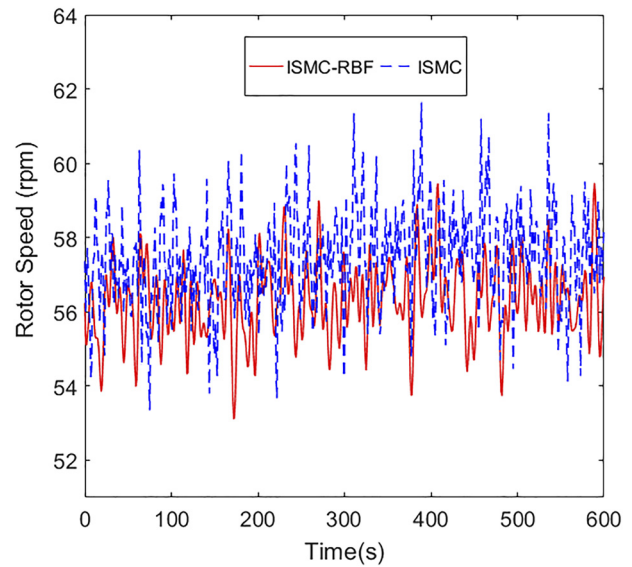


Fig. 3. Time variations of rotor speed

Table 2. Comparison of rotor speed performance

ω_t (rpm)	ISMC	ISMC_RBF
Min	53.1	53.4
Max	61.6	59.3
STD	1.31	1.02

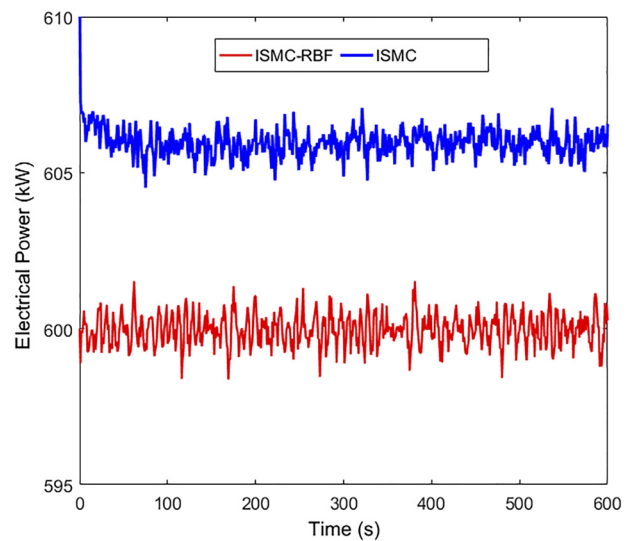


Fig. 4. Time variations of electrical power



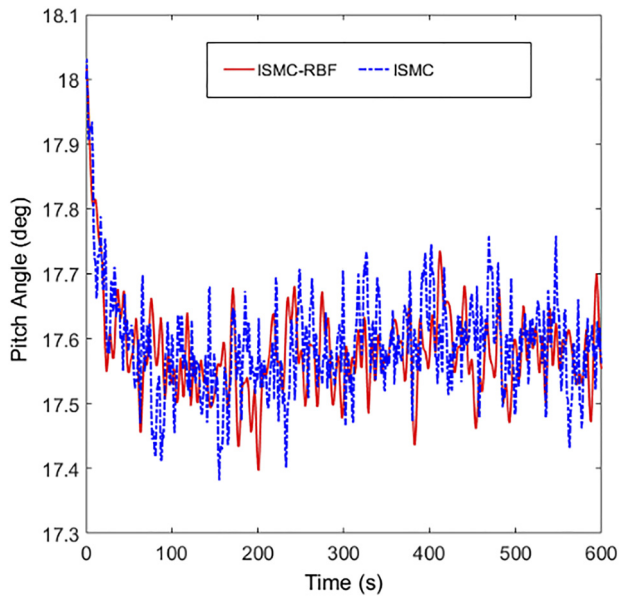


Fig. 5. Time variations of pitch angle

Table 3. Comparison of electromagnetic torque performance

T_{em} (kN.m)	ISMC	ISMC-RBF
Min	24.7	23.6
Max	31.3	29.5
STD	0.088	0.072

0.072 kN.m for ISMC-RBF controller. These results indicate that the proposed controller can better minimize the mechanical loads than the ISMC controller. Combination of RBF with SMC has proven to be effective in rejecting disturbances and enhancing quality of control. These theoretical results need however to be validated by performing experimental tests. The hybrid controller can also be considered to maximize energy extraction in the below rate power regime.

4. CONCLUSION

The simulation carried out in this paper showed a better performance of the hybrid controller that was proposed, ISMC-RBF, for high wind speed regime in the case of horizontal wind turbines that are modeled by a two masses oscillator. The obtained results have shown that RBF neural network is a good estimator that facilitates the command of this uncertain system. The ISMC-RBF adaptive hybrid controller has shown acceptable performances in terms of limiting and stabilizing electrical power and rotor speed around their nominal values, while minimizing torque fluctuations.

REFERENCES

- [1] X. Yin, W. Zhang, Z. Jiang, and L. Pan, "Adaptive robust integral sliding mode pitch angle control of an electro-hydraulic servo pitch system for wind turbine," *Mech. Syst. Signal Process.*, vol. 133, 2019, Paper no. 105704.
- [2] B. Boukhezzer, L. Lupu, H. Siguerdidjane, and M. Hand, "Multi-variable control strategy for variable speed, variable pitch wind turbines," *Renew. Energy*, vol. 32, no. 8, pp. 1273–1287, 2007.
- [3] E. J. Novaes Menezes, A. M. Araújo, J. S. Rohatgi, and P. M. González del Foyo, "Active load control of large wind turbines using state-space methods and disturbance accommodating control," *Energy*, vol. 150, pp. 310–319, 2018.
- [4] V. Kállai, G. L. Szepesi, and P. Mizsey, "Dynamic simulation control in a cryogenic distillation column," *Pollack Period.*, vol. 15, no. 3, pp. 91–100, 2020.
- [5] H. Habibi, H. Rahimi Nohooji, and I. Howard, "Adaptive PID control of wind turbines for power regulation with unknown control direction and actuator faults," *IEEE Access*, vol. 6, pp. 37464–37479, 2018.
- [6] Z. Wang, Z. Shen, C. Cai, and K. Jia, "Adaptive control of wind turbine generator system based on RBF-PID neural network," in *Proc. Int. Jt. Conf. Neural Networks*, Beijing, China, July 6–11, 2014, pp. 538–543.
- [7] X. X. Yin, Y. G. Lin, W. Li, Y. J. Gu, P. F. Lei, and H. W. Liu, "Adaptive back-stepping pitch angle control for wind turbine based on a new electro-hydraulic pitch system," *Int. J. Control*, vol. 88, no. 11, pp. 2316–2326, 2015.
- [8] Q. Yang, X. Jiao, Q. Luo, Q. Chen, and Y. Sun, "L1 adaptive pitch angle controller of wind energy conversion systems," *ISA Trans.*, vol. 103, pp. 28–36, 2020.
- [9] F. Hajdu, P. Szalai, P. Mika, and R. Kuti, "Parameter identification of a fire truck suspension for vibration analysis," *Pollack Period.*, vol. 14, no. 3, pp. 51–62, 2019.
- [10] M. Abolvafoei and S. Ganjefar, "Maximum power extraction from a wind turbine using second-order fast terminal sliding mode control," *Renew. Energy*, vol. 139, pp. 1437–1446, 2019.
- [11] E. El Mjabber, A. El Hajjaji, and A. Khamlichi, "An adaptive control for a variable speed wind turbine using RBF neural network," in *International Conference on Structural Nonlinear Dynamics and Diagnosis*, Marrakech, Maroc, May 23–25, 2016, MATEC Web of Conferences, vol. 83, 2016, Paper no. 09007.
- [12] E. K. El Mjabber, A. El Hajjaji, and A. Khamlichi, "Analysis of a RBF neural network based controller for pitch angle of variable-speed wind turbines," *Proced. Eng.*, vol. 181, pp. 552–559, 2017.
- [13] M. Abolvafoei and S. Ganjefar, "Maximum power extraction from wind energy system using homotopy singular perturbation and fast terminal sliding mode method," *Renew. Energy*, vol. 148, pp. 611–626, 2019.
- [14] J. Liu, *Radial Basis Function (RBF) Neural Network Control for Mechanical Systems*. Berlin Heidelberg: Springer-Verlag, 2013.
- [15] B. Boukhezzer and H. Siguerdidjane, "Nonlinear control of a variable-speed wind turbine using a two-mass model," *IEEE Trans. Energy Convers.*, vol. 26, no. 1, pp. 149–162, 2011.

